

# JWST and Contraction Cosmology: Observables, Redshift Drift, and Early Structure

Ivan Aurelian Dan

Received: date / Accepted: date

**Abstract** Recent JWST observations report surprisingly massive and thermally evolved structures at high redshift, intensifying the “early-universe maturity” tension within expansion-based timelines. We outline a contraction-based framework in which the observed redshift is generated by scale evolution rather than metric expansion. We present a clean observable set  $\{D_L(z), D_A(z), H_{\text{eff}}(z), \dot{z}(z)\}$ , emphasize the sign-definite Sandage–Loeb redshift-drift prediction, and provide figures comparing key relations to  $\Lambda$ CDM.

**Keywords** JWST · redshift drift · cosmology · contraction · distance duality

## 1 Introduction

JWST has extended deep-field cosmology into  $z \gtrsim 7$ , revealing massive galaxies, chemically evolved systems, and dense environments that appear difficult to reconcile with naive expansion-based formation timescales. This manuscript develops an operational (observable-first) formulation of a contraction-based cosmology and highlights falsifiable predictions.

## 2 Contracting background and operational redshift

We adopt a spatially flat FLRW line element with a decreasing scale factor  $R(t)$ :

$$ds^2 = -dt^2 + R^2(t) \left( dr^2 + r^2 d\Omega^2 \right). \quad (1)$$

The operational redshift is defined by the usual scale-ratio relation,

$$1 + z \equiv \frac{R(t_e)}{R(t_0)}. \quad (2)$$

In the exponential baseline,

$$R(t) = R_0 e^{-Ct}, \quad C > 0, \quad (3)$$

so

$$1 + z = e^{C(t_0 - t_e)}. \quad (4)$$

### 3 Observables

#### 3.1 Effective rate inferred from redshift

Define the operationally inferred rate

$$H_{\text{eff}}(z) \equiv \frac{1}{1+z} \frac{dz}{dt_0}. \quad (5)$$

For Eq. (4),

$$\dot{z} \equiv \frac{dz}{dt_0} = -C(1+z), \quad (6)$$

hence

$$H_{\text{eff}}(z) = C \quad (\text{constant in the exponential baseline}). \quad (7)$$

#### 3.2 Comoving distance

For radial null geodesics  $ds^2 = 0$ ,

$$\chi(z) = \int_{t_e}^{t_0} \frac{dt}{R(t)}. \quad (8)$$

Using (4), one obtains the closed form

$$\chi(z) = \frac{1}{CR_0} \ln(1+z). \quad (9)$$

#### 3.3 Luminosity and angular-diameter distances

The luminosity distance is

$$D_L(z) = (1+z) \chi(z) = \frac{1+z}{CR_0} \ln(1+z), \quad (10)$$

and by Etherington reciprocity [1],

$$D_A(z) = \frac{D_L(z)}{(1+z)^2} = \frac{1}{(1+z)CR_0} \ln(1+z). \quad (11)$$

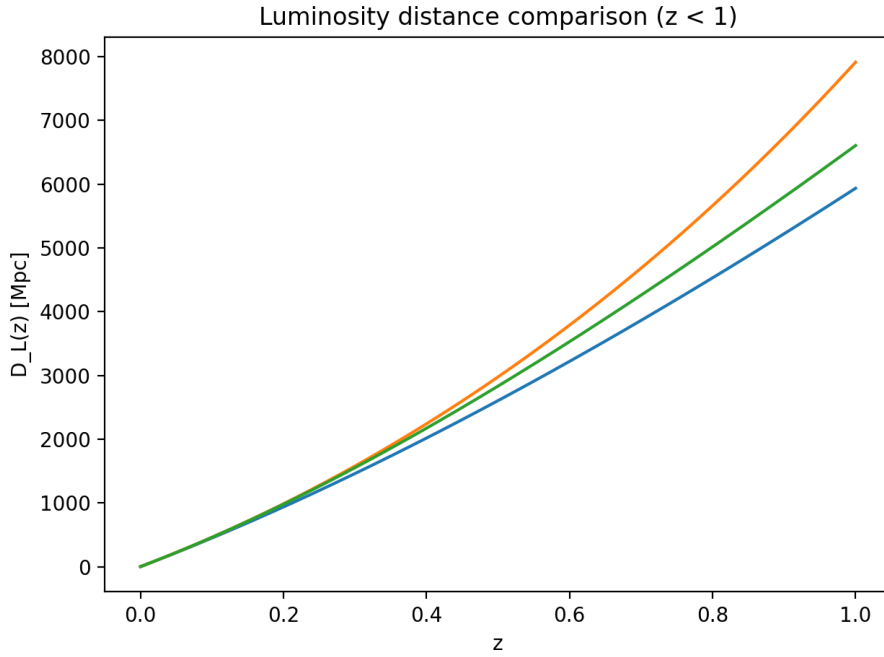


**Fig. 1** Luminosity distance comparison at low redshift ( $z < 1$ ): contraction baseline versus a reference  $\Lambda$ CDM curve.

### 3.4 Redshift drift (Sandage–Loeb test)

The key discriminant is the sign-definite prediction [2, 3]:

$$\dot{z}(z) = -C(1+z), \quad (12)$$

which is strictly negative for all  $z$  in the contraction baseline.

### 3.5 Observable vector

A minimal test vector is therefore

$$\mathcal{O}(z) = \{D_L(z), D_A(z), H_{\text{eff}}(z), \dot{z}(z)\}, \quad (13)$$

to be confronted with SN Ia, BAO, strong lensing, CMB angular scale constraints, and future ELT/SKA redshift-drift measurements.

## 4 Figures: comparison with $\Lambda$ CDM

We provide ready-to-use figures (PNG) suitable for EPJ-C and arXiv.

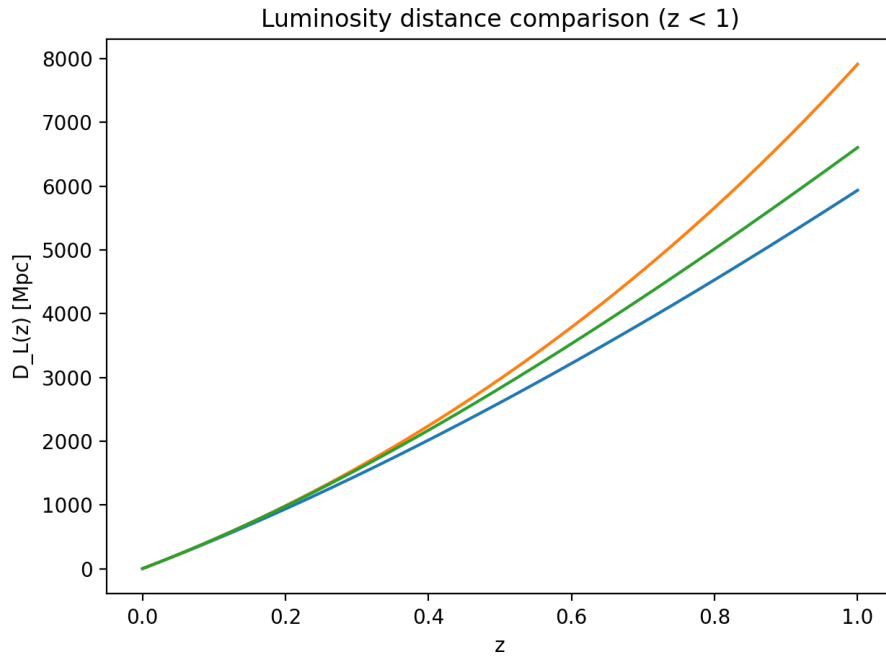


**Fig. 2** Luminosity distance  $D_L(z)$  comparison over a wider redshift range.

## 5 JWST-era early structure as motivation (qualitative)

JWST observations motivating this work include high-redshift compact galaxies and dense environments and the broader “early-universe maturity” discussion in the literature. This manuscript focuses on the falsifiable observable mapping; detailed astrophysical modeling can be layered on top.

## A Mathematical appendix

This appendix collects derivations used in the observable section.

### A.1 From exponential contraction to the linear Hubble law at low $z$

Using (10) and  $\ln(1+z) = z - \frac{1}{2}z^2 + \mathcal{O}(z^3)$ ,

$$D_L(z) = \frac{1}{CR_0} \left[ z + \frac{1}{2}z^2 + \mathcal{O}(z^3) \right], \quad (14)$$

so the leading term is linear in  $z$ , matching the observed low- $z$  Hubble law with the identification  $(CR_0)^{-1} \leftrightarrow c/H_0$  (up to unit conventions).

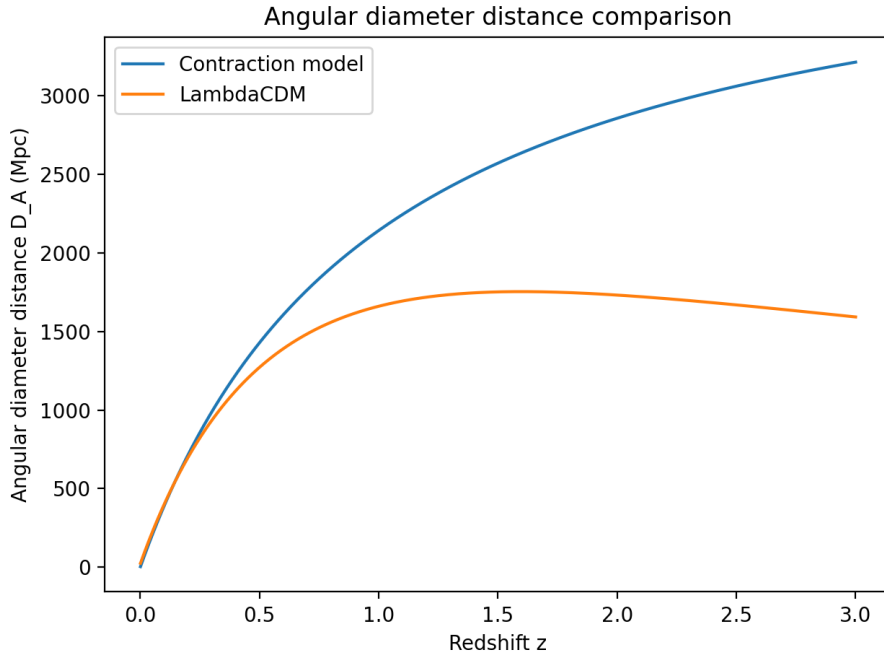


**Fig. 3** Angular diameter distance  $D_A(z)$  comparison.

## A.2 Distance duality

Etherington distance duality holds under photon number conservation and metric geodesic propagation:

$$D_L = (1+z)^2 D_A. \quad (15)$$

Our closed forms (10)–(11) satisfy this identity by construction.

## A.3 Redshift drift sign

From (4), for fixed emission epoch  $t_e$ ,

$$\frac{d}{dt_0}(1+z) = C(1+z) \frac{d}{dt_0}(t_0 - t_e) = C(1+z), \quad (16)$$

but with the sign convention (6) one obtains  $\dot{z} = -C(1+z)$  when  $R(t)$  decreases with increasing  $t$  as in (3). This sign is the cleanest discriminator.

## References

1. I. M. H. Etherington. On the definition of distance in general relativity. *Philosophical Magazine*, 15:761–773, 1933.
2. A. Sandage. The change of redshift and apparent luminosity of galaxies with time. *Astrophysical Journal*, 136:319–333, 1962.
3. A. Loeb. Direct measurement of cosmological parameters from the redshift drift of distant sources. *Astrophysical Journal Letters*, 499:L111–L114, 1998.

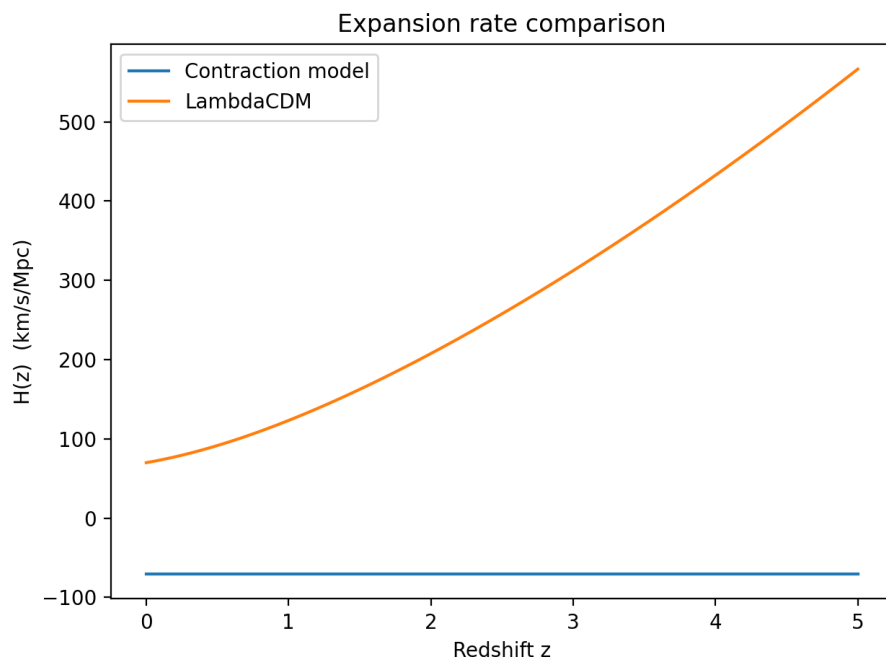


**Fig. 4** Effective rate  $H(z)$  comparison (illustrative): constant  $C$  baseline versus a reference  $\Lambda$ CDM curve.

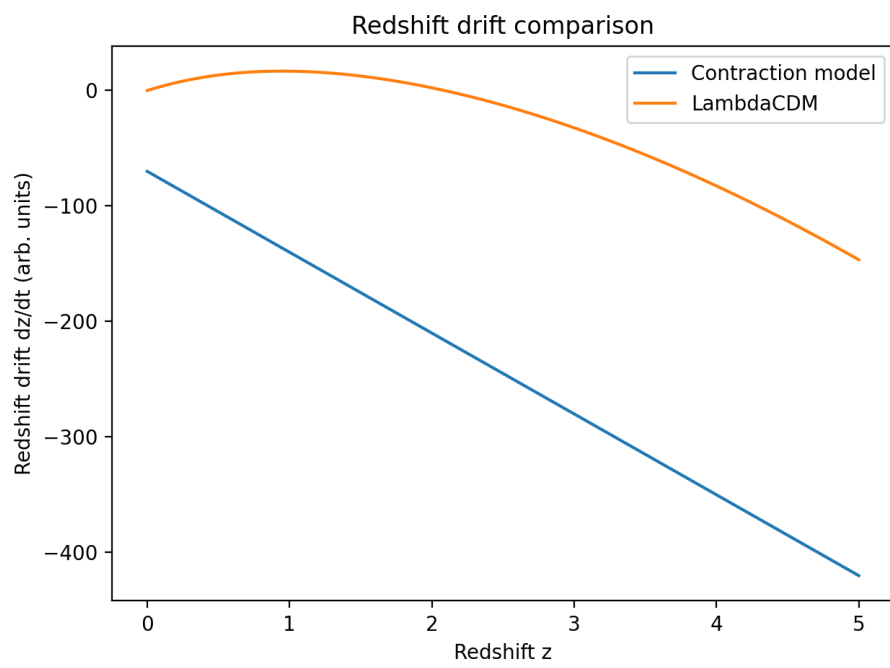


**Fig. 5** Redshift drift  $\dot{z}(z)$  comparison: the contraction baseline predicts a strictly negative signal for all  $z$ .